Turkish Journal of Chemistry

http://journals.tubitak.gov.tr/chem/

Research Article

Turk J Chem
(2018) 42: 562 – 571

doi:10.3906/kim-1708-41

Physicochemical characterization of different cellulose polymorphs/graphene oxide composites and their antibacterial activity

Sherif Mohamed Abdel Salam KESHK[1,*], **Ibrahim Sayed YAHIA**[2]

[1]Department of Chemistry, College of Science, King Khalid University, Abha, Saudi Arabia

[2]Advanced Functional Materials & Optoelectronic Laboratory, Department of Physics, College of Science, King Khalid University, Abha, Saudi Arabia

Received: 20.08.2017 • **Accepted/Published Online:** 10.01.2018 • **Final Version:** 27.04.2018

Abstract: In order to investigate the interaction of graphene oxide (GO) with different cellulose polymorphs (I and II), we synthesized cellulose (I and II)/GO composites using the sonication method. Interestingly, no new peaks were observed in the FT-IR pattern of the cellulose (I and II)/GO composites, indicating that no chemical reactions took place between GO and cellulose. The X-ray diffraction patterns of cellulose I and II/GO composites were slightly different than those observed for cellulose I and II, indicating that some physical interactions occurred between the GO and cellulose. Unexpectedly the d-spacing values and the diffraction plane at the high-angle side were most likely expanded in cellulose I rather than in cellulose II by adding GO, confirming the highest reactivity of GO toward cellulose I rather than cellulose II. Furthermore, SEM images showed that the conformal coating of GO on cellulose I was larger than that on cellulose II due to the strong adhesion between the GO and cellulose I. Cellulose/GO showed antimicrobial properties, and GO was found to be promising for textile antimicrobial finishing.

Key words: Cellulose I and II, graphene oxide, X-ray diffractometer, composite, antibacterial activity

1. Introduction

There are four different polymorphs of cellulose: I, II, III, and IV.[1] Cellulose I and II are the most studied forms of cellulose. In the fabrication of superhydrophobic and electroconductive textiles, improving the physicochemical characterization of cellulose is a key issue. Chemically, cellulose II shows higher chemical reactivity than cellulose I and can be used to make cellophane. It is considered as one of the most useful fibers and has wide applications in the chemical industry.[2] The crystalline structure of cellulose I in native cellulose can be converted into that of cellulose II by mercerization in sodium hydroxide.[3–5] Mercerization depends on the type and concentration of the alkaline solution, its temperature, treatment time, the tension of the materials, and the additives.[5] During the process of mercerization, all fibers are converted into a swollen state and the assembly and orientation of microfibrils are completely disrupted.[5] The original parallel-chain crystalline structure of cellulose I changes to antiparallel chains of cellulose II. The hydrogen bond in cellulose I is O_2–H—O_6, whereas in cellulose II it is O_2–H—O_6, O_6–H—O_6, and O_2–H—O_2. On the other hand, graphene oxide (GO) with a high oxygen content can be attached to the polymers by their functional groups and bound below or above each plane as well as on the edge of the graphene sheet.[6] The presence of GO with natural polymers enhances the hydrophobic properties of composites, and no other functional group remains on the polymer surface. Further-

*Correspondence: keshksherif@gmail.com

more, GO is accepted as a filler in bioceramic materials owing to the high mechanical constants of the composite obtained.[7] In addition, the nanostructures of cellulose/GO have been documented.[8,9] Results indicated that GO is coated only as the cellulose fabric with enhanced hydrophobic properties, high electrical conductivity, and thermal stability. Furthermore, the nanostructures of cellulose/GO showed no detectable X-ray band due to the presence of GO.[10,11] The mercerization treatment of cellulose is a versatile chemical modification. Moreover, the process of mercerization shows changes in the crystalline structure and many other properties. Most of the investigations conducted on the mercerization of cellulose have focused on whole cellulose fibers, i.e. assemblies of large numbers of organized microfibrils.[4,5] On the other hand, the biological applications of graphene are limited compared to GO due to the chemical structure and properties of GO such as intrinsic luminescence, hydrophilicity, tunable band gap, biocompatibility, and photocatalytic activity, which makes it a suitable material for biological and biomedical applications.[6] GO-coated cellulose shows antibacterial properties and is more toxic to gram-positive than gram-negative bacteria.[6] To the best of our knowledge, no studies have been carried out regarding the reactivity of cellulose I and II crystals toward composite formation with GO and antimicrobial activities (bacteria or fungi) of cellulose II or its composite. The main objective of this study was to evaluate the physicochemical characterization of both cellulose I and II/GO composites in order to obtain the best form of cellulose that can effectively react with GO using Fourier transform infrared spectroscopy (FT-IR) analyses, X-ray diffraction (XRD), and scanning electron microscopy (SEM).

2. Results and discussion

2.1. Fourier-transform infrared spectroscopy of cellulose/GO composites.

Figure 1 presents the measured FT-IR characteristic bands of cellulose I and II and their composites. In the spectra, bands at 4000–2995 cm^{-1}, 2900 cm^{-1}, 1430 cm^{-1}, 1375 cm^{-1}, and 900 cm^{-1} were found to be sensitive to the variations in crystalline and amorphous regions.[5,12] Furthermore, Figure 1 shows a strong hydrogen-bonded OH stretching vibration within the region of 2995–3600 cm^{-1}. The intermolecular hydrogen bonding of O_2–H—O_6 for cellulose I and O_2–H—O_6, O_6–H—O_6, and O_2-H—O_2 for cellulose II was shown at the 3438 cm^{-1}, 3334 cm^{-1}, and 3293 cm^{-1} positions, respectively.[12,13] The absorbance of CH stretching in cellulose I was shifted from 2901 cm^{-1} to a lower wave number at 2890 cm^{-1} in cellulose II (Figure 1), which indicates that different arrangements result in the changes of angles around the β-glycosidic linkage.[2]

The absorbance intensities at 1427 cm^{-1} are assigned to CH_2 bending in cellulose I.[14] The intensity of this peak increases in cellulose II, which reflects a higher number of disordered cellulose structures.[15] The minute change at 1370 cm^{-1} is attributed to different CO stretching vibrations in cellulose I and II fibers.[12] The FT-IR spectra of the cellulose I and II/GO samples were quite similar to those of the original samples. It was observed that no new peaks appeared in the treated samples, indicating that no chemical reactions took place between the GO and cellulose.

2.2. XRD analysis of cellulose/GO composites

The X-ray pattern of the cellulose exhibits the typical diffraction peaks of the crystalline structure of cellulose I at $2\theta = 14.76^\circ$, 15.42°, 22.70°, and 23.14° corresponding to the (1^-10), (110), (002), and (020) planes, respectively. However, cellulose II exhibits diffraction peaks at $2= 12.25^\circ$, 20.38°, and 22.24° corresponding to the (1^-10), (110), and (020) planes, respectively (Figure 2).

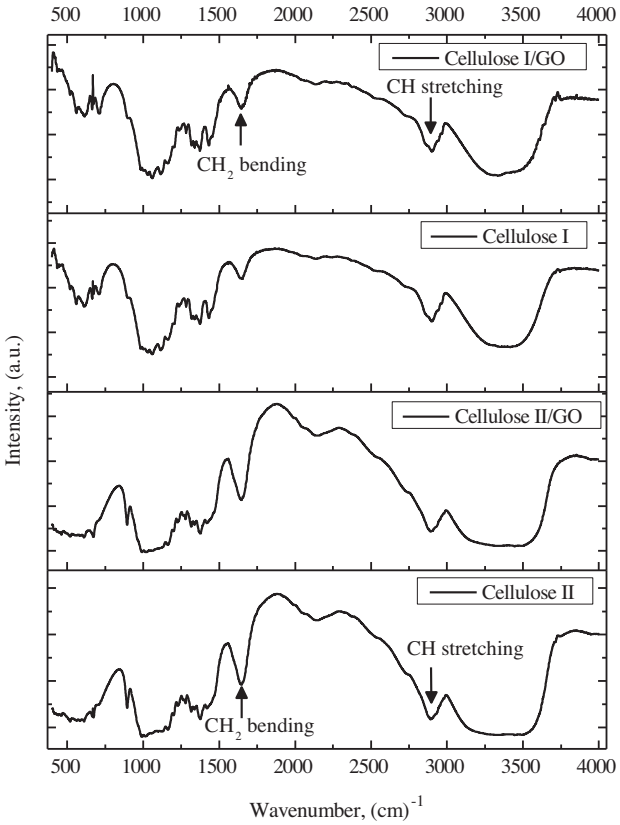

Figure 1. FT-IR spectra of cellulose I and II and their composites.

There are no impurity peaks observed in the XRD patterns of both cellulose composites I and II. In the X-ray diffraction pattern of cellulose (I & II)/GO composites, the peak intensity and crystallinity index were decreased and accompanied by line broadening (Figures 2 and 3). Therefore, GO was effectively inserted in the cellulose fibers and the crystallinity index was decreased due to the loss of the packing order of glucopyranose rings.[5]

Although the X-ray diffraction patterns of the cellulose (I and II)/GO composites were different than those observed for cellulose I and II, there were significant differences in the values of d-spacing (Table 1). The d-spacing values showed that the diffraction plane on the high-angle side was most likely expanded by adding GO between the cellulose sheets corresponding to the (020) plane at $2\theta = 22.86^\circ$ In addition, a broad weak peak from the graphene oxide at $2\theta = 10.5^\circ$ corresponding to the (002) plane can be detected in the cellulose I/GO composite (Figures 2 and 3). However, the X-ray diffraction patterns of the cellulose II/GO composites showed slightly different d-spacing values than those of cellulose II, indicating that GO reacts more effectively with cellulose I than cellulose II. These results can be explained by the formation of the hydrogen bond in both cellulose composites I and II. Both intra- and intermolecular hydrogen bonding occurs in cellulose. In cellulose I, the presence of intramolecular hydrogen bonds is of high relevance considering the single-chain conformation and stiffness. The Scheme presents the existence of hydrogen bonds between O-3-H and O-5 (2.75 Å) of the adjacent glucopyranose unit and O-2-H and O-6 (2.87 Å) of the native crystalline cellulose.[16]

In cellulose II crystallites, the hydrogen bonds are essentially the same as those proposed for cellulose I,

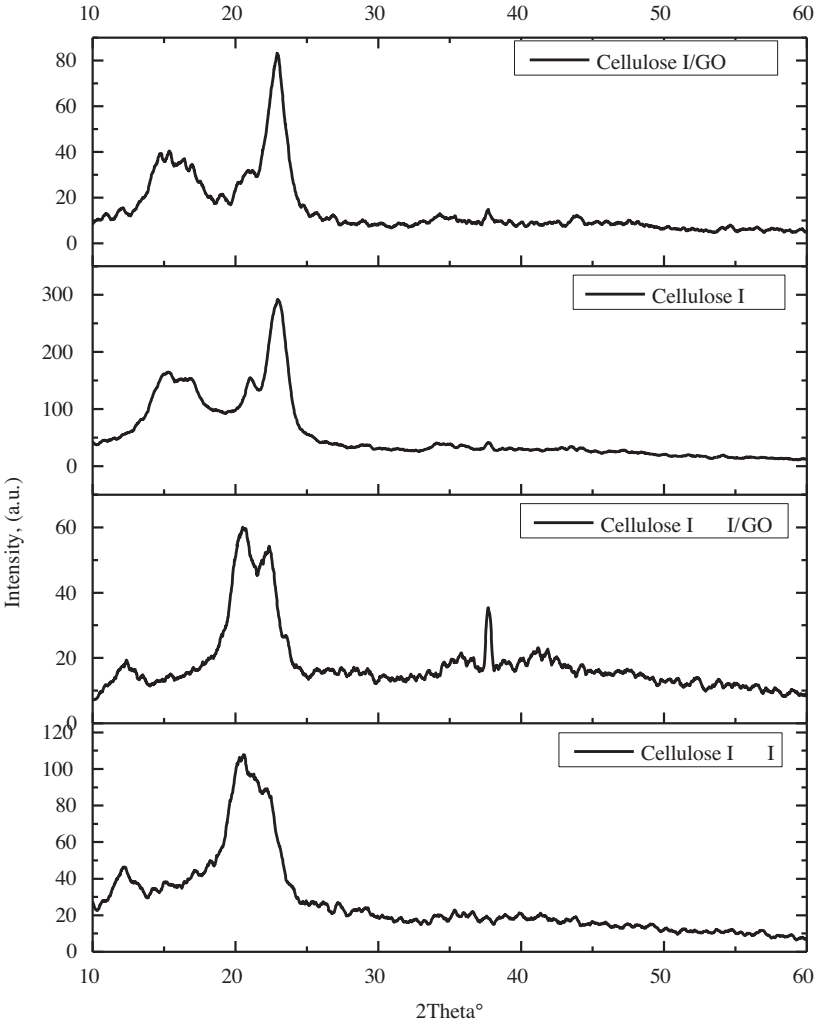

Figure 2. X-ray pattern of cellulose I and II and their composites.

Table 1. The X-ray diffraction data of cellulose I and II and their composites.

Samples	$2\theta^{\circ}/d$ (1-10)	$2\theta/d$ / d (110)	$2\theta/d$ / d (020)
Cellulose I	14.76 (5.99)	15.42 (5.74)	23.14 (3.84)
Cellulose II	12.11 (7.30)	20.30 (4.37)	22.54 (3.94)
Cellulose I/GO	14.97 (5.88)	16.34 (5.39)	22.86 (3.94)
Cellulose II/GO	12.25 (7.25)	20.38 (4.35)	22.24 (3.98)

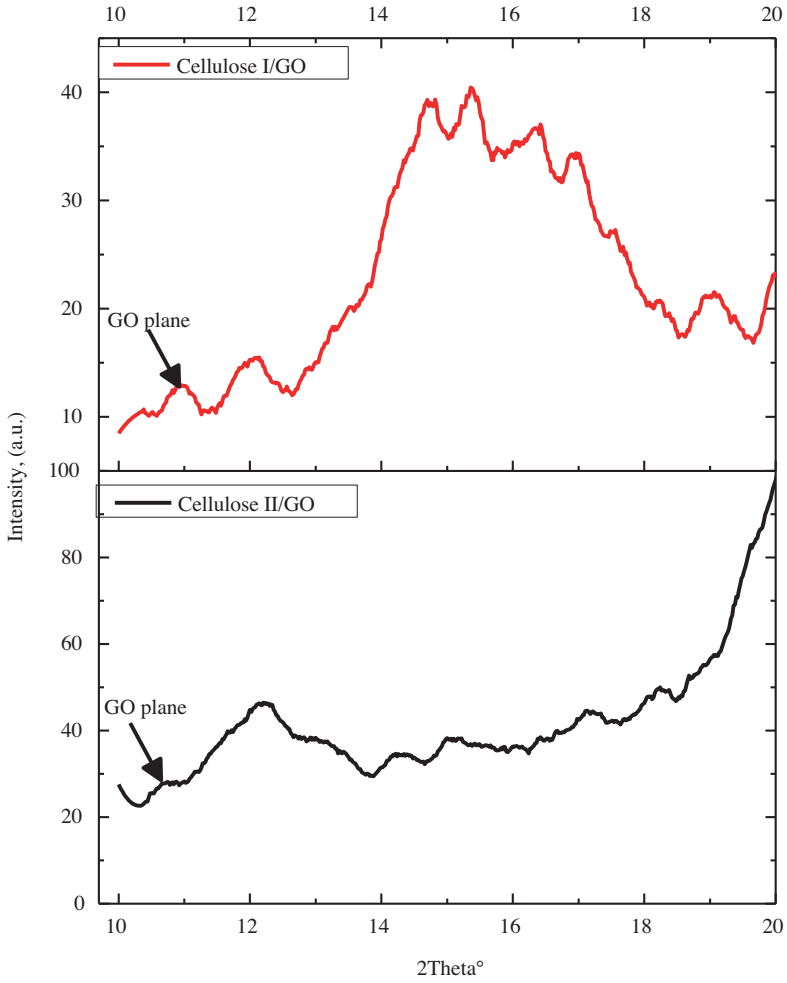

Figure 3. X-ray pattern magnification of cellulose I and II and their composites.

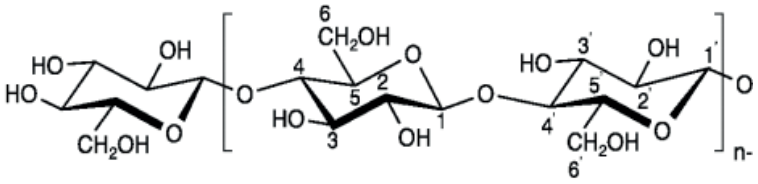

Scheme. Molecular structure of cellulose.

but they are shorter than cellulose I (2.69 Å) when O-3-H and O-5 are considered.[17] Thus, the intermolecular hydrogen bonding in cellulose II is significantly strong compared to that in cellulose I. The antiparallel chain model (cellulose II) enables the formation of not only interchain but also of interplane hydrogen bonds.[18] Therefore, GO can more easily react with cellulose I than cellulose II. The interaction between GO and cellulose can be explained as follows: GO has various functional groups, such as carboxyl, carbonyl, hydroxyl, and epoxy groups, that make it hydrophilic in nature.[19,20] The hydrophilicity of GO allows it to be readily soluble in water at molecular levels with high surface capacity for adsorption, strongly adhering to the surface of cotton fabrics during the reaction time. This strong adhesion of GO onto the surface of the cellulose is confirmed by

the X-ray diffractograms of cellulose and cellulose/GO composites as shown in Figure 3. The crystallite widths of cellulose I and its composites were found to be 2.55 nm and 3.01 nm, respectively. However, the crystallite widths of cellulose II and its composites were found to be 2.34 nm and 2.44 nm, respectively.

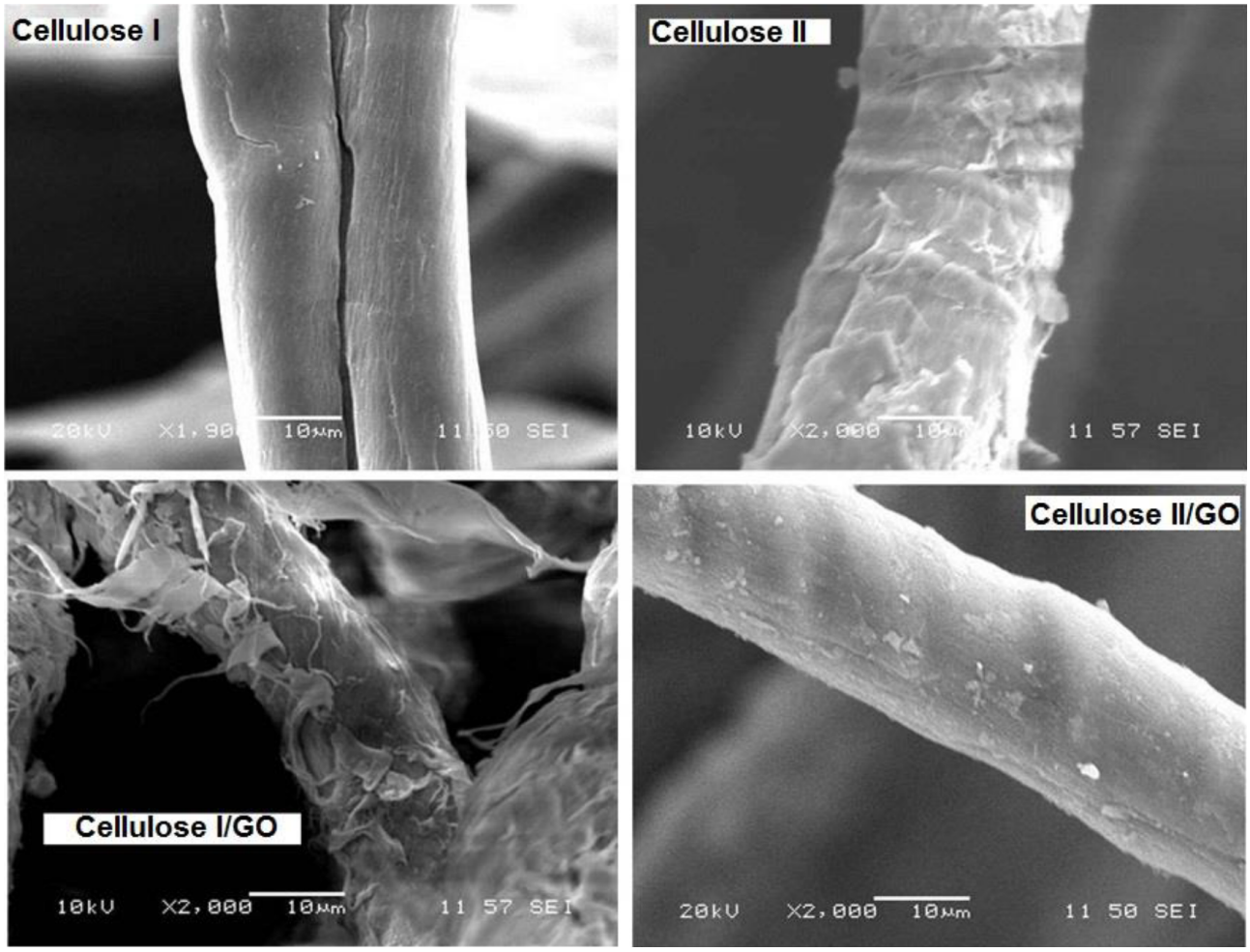

Figure 4. SEM micrographs of cellulose I and II and their composites.

2.3. SEM analysis of cellulose/GO composites

Figures 4a–4d show the SEM images of cellulose I, cellulose II, and their composites with GO. From this figure, the existence of a GO peel dispersed homogeneously through the whole matrix of cellulose I rather than cellulose II is clear. Compared to cellulose I and II, a notable change in the surface morphology of cellulose I was observed in the presence of GO. The high-magnification image demonstrates a smoother surface of the cellulose I/GO owing to the conformal coating of GO. The conformal coating was mainly caused by the GO peel, and the size uniformity of graphene together with the strong adhesion between the graphene and cellulose I fibers confirms that GO is uniformly coated on it. However, nonsignificant coating in cellulose II/GO could be observed due to the low interaction between cellulose II and GO. The same results for a bacterial cellulose/GO composite were observed, where the GO peel was tightly covered on the bacterial cellulose skeleton (cellulose I).[21]

2.4. Antimicrobial activity of cellulose (I & II)/GO composites

The antimicrobial activity of cellulosic fiber and cellulose (I & II)/GO composites was tested against gram-negative bacterium *Escherichia coli* and gram-positive bacterium *Staphylococcus aureus*. Table 2 shows the values of microbial reduction for both samples. Cellulosic fabric loaded with GO exhibited good antibacterial activity against *E. coli*. On the other hand, cellulose (I & II)/GO composites provided a maximum microbial reduction in the case of *E. coli* and *C. albicans* ($R = 99.9\%$) and slightly lower microbial reduction in the case of *S. aureus* ($R = 99.6\%$). In another study, the antibacterial activity of GO-coated cotton fabric was examined only against gram-negative bacteria (*E. coli* DH5a) and gram-positive bacteria (*S. iniae*).[6] The experimental results revealed that the cellulose I/GO composite was effective toward gram-positive bacteria only.[6] Our synthesized cellulose I and II/GO composites showed antimicrobial properties for both gram-positive and -negative bacteria, indicating the greater effectiveness of the method in inserting GO into cellulose planes than earlier reported.[6] Therefore, GO can be used in textile antimicrobial finishing by applying our method.

Table 2. Microbial activities of cellulose I and II and their composites.

Sample	Organism	Medium	Condition	Temp.	Incub.	Activity
Cellulose I	*S. aureus* (ATCC 2592)	Mueller Hinton agar	Aerobic	37 °C	36 h	+ve
Cellulose II	*S. aureus* (ATCC 2592)	Mueller Hinton agar	Aerobic	37 °C	36 h	+ve
Cellulose I/GO	*E. coli* (ATCC 2592)	Mueller Hinton agar	Aerobic	37 °C	36 h	-ve
Cellulose II/GO	*E. coli* (ATCC 2592)	Mueller Hinton agar	Aerobic	37 °C	36 h	-ve
Cellulose I/GO	*C. albicans* (ATCC 1023)	Sabouraud dextrose agar	Aerobic	30 °C	36 h	-ve
Cellulose II/GO	*C. albicans* (ATCC 1023)	Sabouraud dextrose agar	Aerobic	30 °C	36 h	-ve

2.5. Conclusions

In this study, we prepared certain cellulose (I & II)/GO composites by using a simple and effective method without applying any other toxic cross-linking agents. Cellulose I showed higher reactivity toward GO than cellulose II. On the other hand, both cellulose I/GO and cellulose II/GO showed negative reactivity toward microbial testing. Therefore, we conclude that these results will open a new medical trend for cotton applications in future.

3. Experimental

3.1. Chemicals

All chemicals used in this study were purchased from Sigma-Aldrich, were of analytical grade, and were used without any further purification/treatment. The cotton linter (DP = 900–920) was also purchased from Sigma.

3.2. Preparation of GO

Graphite powder (5 g) was added to a 1-L glass beaker followed by the addition of 115 mL of conc. sulfuric acid. The above solution was stirred on a magnetic stirrer for 30 min. After that, 2.5 g of sodium nitrate was added slowly. The above beaker was fixed in an ice container for 30 min and then its temperature was brought to room temperature. Further, 15 g of potassium permanganate was gradually added to this solution and stirred at 40 °C for 2 h until a thick paste was obtained. Distilled water (500 mL) was added slowly and carefully to the above solution, as conc. sulfuric acid was present. The final solution was stirred again for 1 h. To terminate the reaction 10 mL of hydrogen peroxide (30%) was added with continuous stirring for a further 2 h. The color of the obtained solution was brown. Inorganic anions and impurities were removed by washing using centrifuge and ultrasonication methods. After drying at 70 °C for 48 h, we obtained GO in powder form. Different concentrations of GO in 500 mL of distilled water were dispersed by using a high-power ultrasonic system at 200 W for 15 min.[6]

3.3. Cellulose II preparation

The cotton linter was prepared by immersing it in 20% NaOH for 1 week at room temperature. Then the fibers were filtered and washed with fresh water until all NaOH was removed.[3,22]

3.4. Preparation of cellulose/GO composites

The cellulose (I & II) composites were immersed in 20 mL of GO (0.01 g) solution and stirred for 2 h. Then ultrasonication was used to complete the synthesis. The sample was dried at room temperature.

3.5. FT-IR spectroscopy

Following the protocols suggested by Abbott et al., FT-IR spectroscopy (Bruker IFS 66) was performed.[23]

3.6. X-ray diffraction

The X-ray diffraction patterns of cellulose (I and II) and its composites with GO were determined using a Shimadzu-Lab-XRD-6000 diffractometer with nickel-filtered Cu Kα radiation at 40 kV and 50 mA.

3.6.1. Determination of crystallinity index

The crystallinity index (CI) was calculated from the diffracted intensity data using the method reported by Segal et al.[24] The CI calculation was performed using Eq. (1):

$$CI\% = \frac{I_{020} I_{am}}{I_{020}} \times 100, \tag{1}$$

where I_{020} is the maximum intensity at $2\theta 22.8^{\circ}$ and I_{am} is the intensity of the amorphous background scatter measured at $2\theta = 18^{\circ}$

3.6.2. Crystallite widths (L)

The crystallite widths of cellulosic fibers were estimated and evaluated using the Scherer equation (Eq. (2)). In order to evaluate the width of the crystallites, the Scherrer equation with a constant (K) equal to 0.9 at the

half-width peak of the (200) plane at $2\theta = 22.8^\circ$ was applied:[25,26]

$$\lambda L = k/\beta \cos\theta, \tag{2}$$

where L is the crystallite width, θ is the Bragg angle, λ is the wavelength of the radiation, K is a constant, and β is the corrected width of the peak given by the specimen.

3.7. Scanning electron microscopy

The morphology of cellulose composites I and II was examined by using field emission scanning electron microscopy (FESEM) images obtained by a FESEM JEOL 6340 electron microscope equipped with an energy-dispersive X-ray analysis instrument (EDX), used to investigate the elemental composition of the system.

4. Bacterial and fungal strains

In this study, bacterial and fungal strains collected from frozen stocks at King Khalid University were used. To prepare 0.5 McFarland standard suspensions, one to three loopfuls of cultures 24 h old from each test strain were used. As recommended by the Clinical and Laboratory Standards Institute, Mueller Hinton agar (DIFCO) plates were used in the in vitro antimicrobial testing. Then the impregnated dried cotton was placed on the inoculated agar. Finally, the inoculated plates were incubated at 37 °C and examined after 24, 48, and 72 h for inhibition zones under and around it.

Acknowledgment

The authors would like to thank the Deanship of Scientific Research at King Khalid University for funding this work through a general research project under Grant Number G.R.P-12-38.

References

1. Cai, G.; Xu, Z.; Yang, M.; Tang, B.; Wang, X. *Appl. Surf. Sci.* **2017**, *393*, 441-448.
2. Ciacco, G. T.; Morgado, D. L.; Frollini, E.; Possidonio, S.; El Seoud, O. A. *J. Brazil. Chem. Soc.* **2010**, *21*, 71-77.
3. Keshk, S. M. A. S; Mohamed G. In *Science and Principles of Biodegradable and Bioresorbable Medical Polymers - Materials and Properties*; Zhang, X., Ed. Elsevier: Amsterdam, the Netherlands, 2017, p. 232.
4. Keshk, S. M. A. S. *Carbohyd. Polym.* **2015**, *115*, 658-662.
5. Sensale-Rodriguez, B.; Rafique, S.; Yan, R.; Zhu, M.; Protasenko, V.; Jena, D. *Opt Express.* **2013**, *21*, 2324-2330.
6. Karthikeyan, K.; Umasuthan, N.; Rajneesh, M.; Jehee, L.; Sang-Jae, K. *Appl. Nanosci.* **2012**, *2*, 119-126.
7. Lahiri, D; Benaduce, A.; Kos, L.; Agarwal, A. *Nanotechnology* **2011**, *22*, 355702.
8. Krishnamoorthy, H. N. S.; Jacob, Z.; Narimanov, E.; Kretzschmar, I.; Menon, V. M. *Science* **2012**, *336*, 205-209.
9. Shateri-Khalilabad, M; Yazdanshenas, M. *The Journal of the Textile Institute* **2013**, *104*, 861-869.
10. Tissera, N. D.; Wijesena, R. N.; Perera, J. R.; Nalin de Silva, K. M.; Amaratunge, G. A. J. *Appl. Surf. Sci.* **2015**, *324*, 455-463.
11. Tang, X.; Tian, M.; Qu, L.; Zhu, S.; Guo, X.; Han, G.; Sun, K.; Hu, X.; Wang, Y.; Xu, X. *Synth. Met.* **2015**, *202*, 82-88.
12. Oh, S. Y.; Yoo, D. I.; Shin, Y.; Seo, G. *Carbohyd. Res.* **2005**, *340*, 417-428.
13. Langan, P.; Nishiyama, Y.; Chanzy, H. *J. Am. Chem. Soc.* **1999**, *121*, 9940-9946.

14. El-Wakil, N. A.; Hassan, M. L. *J. Appl. Polym. Sci.* **2008**, *109*, 2862-2871.

15. Krebs, F. C. *Sol. Energ. Mat. Sol. C* **2008**, *92*, 685-685.

16. Sarko, A.; Muggli, R. *Macromolecules* **1974**, *7*, 486-494.

17. Kolpak, F. J.; Blackwell, J. *Macromolecules* **1976**, *9*, 273-278.

18. Gautam, S. P.; Bundela, P. S.; Pandey, A. K.; Jamaluddin, M. K.; Sarsaiya, S. *Journal of Applied and Natural Sciences* **2010**, *2*, 330-343.

19. Karthikeyan, A.; Sudha, M.; Pandiyan, M.; Senthil, N.; Shobhana, V.G.; Nagarajan, P. *Int. J. Plant Pathol.* **2011**, 2, 115-125.

20. Si, Y.; Samulski, E. T. *Nano Lett.* **2008**, *8*, 1679-1682.

21. Fang, Q.; Zhou, X.; Deng, W.; Zheng Z.; Liu, Z. *Scientific Reports* **2016**, *6*, 1-11.

22. Keshk, S. M. A. S.; Abd-Rabboh, H. S. M.; Hamdy, M. S.; Badr, I. H. In *18th International Conference on Applied Chemistry*; Zurich, Switzerland; January 2016.

23. Keshk, S. M. A. S. *Carbohyd. Polym.* **2008**, *74*, 942-945.

24. Segal, L.; Creely, J. J.; Martin, A. E. Jr; Conrad, C. M. *Text. Res. J.* **1959**, 29, 786-794.

25. Jasiukaityte, E.; Kunaver, M.; Poljansek, I. *BioResources* **2012**, *7*, 3008-3027.

26. Keshk, S. M. A. S.; Yousef, E.; Omran, A. *Indian Journal of Fiber and Textile Research* **2015**, *40*, 190-195.